KSTLE International Journal, Vol. 5, No. 2, December 2004, pp. 52-56

Modified Boundary-Fitted Coordinate System Method for HDD Slider Analysis

Pyung Hwang† and Polina V. Khan*

Professor, School of Mechanical Engineering, Yeungnam University, Korea
**Graduate Students, Department of Mechanical Engineering, Yeungnam University, Korea*

Abstract: The hard disk drive performance depends strongly on air bearing characteristics of the head slider. The objective of the slider design is to provide accurate positioning of the magnetic read/write element at the very small height above the disk. Application of the numerical methods is required due to complexity of the air bearing surface of the slider. The Boundary-Fitted Coordinate System Divergence Formulation method can be used for calculation of pressure distribution in the case of steep film thickness gradients. In the present work, the interpolating functions used in the expression for the Couette flow are modified in order to improve the solution characteristics in the extremely high compressibility number region. The advantages of the modified method are demonstrated on example of the flat skewed slider. Finally, the modi.ed method is applied to analysis of the static characteristics of the femto-slider. The analysis results indicate the effect of the slider's air bearing surface crown on the flying height and the pitching angle in steady state position.

Key words: Hard Disk Drive Air Slider, Boundary-Fitted Coordinate System, Divergence Formulation, Upstream Scheme, Static Analysis

Introduction

The main computer data storage, such as the hard disk drive has several heads (sliders) and disks. The magnetic reading/writing elements are mounted on the slider that flies above the disk under the action of suspension force and air bearing force. Increasing the areal storage density required decreasing the flying height.

The numerical methods provide useful instrument for the slider air bearing design. The Boundary-Fitted Coordinate System Divergence Formulation method (BFCS DF method) [1] allows calculation of the air bearing pressure for the slider with complicated boundary conditions. The convective (Couette) flow terms in the dimensionless Reynolds' equation are proportional to compressibility number (Λ) that is rapidly increased with decreasing the flying height [2]. Therefore, high compressibility number region corresponds to the convection dominated flow. Practically any numerical method, applied to analysis of the convection dominated flow, must utilize the upstream approach in order to avoid the artificial waviness of the solution [3,4,5,6]. In the BFCS DF method [1,6], the high-amplitude discontinuity in the direction of the Couette flow was successfully suppressed, by the mean of the upstream scheme. However, the much smaller discontinuity in the transverse direction remained, and became significant with further increasing of compressibility number in HDD slider analysis problems. In the present work, the transverse discontinuity in the solution is eliminated by modifying the BFCS DF method. First, the performance of the original and modified BFCS DF methods are compared for the simple slider model. After this, the static analysis of the femto slider is conducted by using the modified method.

†Corresponding author: Tel: 82-53-810-2448, Fax: 82-53-810-4627
E-mail: phwang@yumail.ac.kr

Fundamental Equations

The pressure distribution in the air film between slider and disk is described by the Reynolds equation for isothermal compressible flow that has the dimensionless form [2]

$$\frac{\partial}{\partial X}\left(H^3\varphi P\frac{\partial P}{\partial X}\right)+\frac{\partial}{\partial Y}\left(H^3\varphi P\frac{\partial P}{\partial Y}\right)=\Lambda\left(\frac{\partial}{\partial X}(PHU)+\frac{\partial}{\partial Y}(PHV)\right), \tag{1}$$

where $(X, Y) = (x, y)/b$ are dimensionless coordinates, $P = p/p_0$ is the dimensionless pressure, $H = h/h_0$ is the dimensionless film thickness, φ is the Poiseuille flow rate coefficient accounting for the air rarefaction effect, $\Lambda = 6u_0\eta b/(p_0h^2_0)$ is the compressibility number, and $(U, V) = (u_x, u_y)/u_0$ is the dimensionless disk surface velocity.

The Reynolds equation (1) is equivalent to the mass conservation law

$$\frac{\partial q^x}{\partial X}+\frac{\partial q^y}{\partial Y}=0, \tag{2}$$

where

$$q^x=-H^3\varphi P\frac{\partial P}{\partial X}+\Lambda PHU, \tag{3a}$$

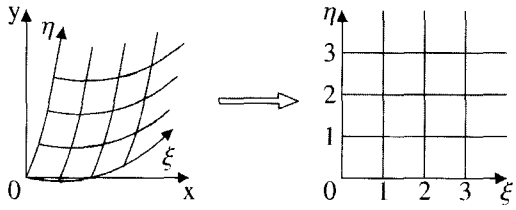

Fig. 1. Physical and computational domains.

$$q^{v} = -H^3 \varphi P \frac{\partial P}{\partial Y} + \Lambda PHV. \tag{3b}$$

In order to describe the boundary conditions correctly, the mesh in the physical domain is drawn so that mesh lines follows the film thickness steps boundaries. Such mesh is called the Boundary-Fitted Coordinate System. The discretization is easier, if in the computational domain the mesh is rectilinear with equidistant nodes position (Fig. 1). The local coordinate transformation parameters x_ξ, x_η, y_ξ, y_η are defined as following

$$\begin{pmatrix} dx \\ dy \end{pmatrix} = \begin{pmatrix} x_\xi & x_\eta \\ y_\xi & y_\eta \end{pmatrix} \cdot \begin{pmatrix} d\xi \\ d\eta \end{pmatrix}. \tag{4}$$

The mass fluxes in the computational domain are given by the following equations

$$Q^{\xi} = \int_{\eta_1}^{\eta_2} (-AP_\xi + BP_\eta + DP) d\eta, \tag{5a}$$

$$Q^{\eta} = \int_{\xi_1}^{\xi_2} (BP_\xi - CP_\eta + EP) d\xi, \tag{5b}$$

where

$$\begin{aligned} &A = H^3 \varphi(\alpha/J), \\ &B = H^3 \varphi(\beta/J), \\ &C = H^3 \varphi(\gamma/J), \\ &D = \Lambda H(Uy_\eta - Vx_\eta), \\ &E = \Lambda H(-Uy_\xi + Vx_\xi), \\ &\alpha = x_\eta^2 + y_\eta^2 \\ &\beta = x_\eta x_\xi + y_\eta y_\xi \\ &\gamma = x_\xi^2 + y_\xi^2 \\ &J = x_\xi x_\eta - y_\xi y_\eta \end{aligned} \tag{6}$$

In Eq. (5), the terms with coefficients A, B and C express the Poiseuille flow, and the terms with coefficients D and E express the Couette flow.

The control volume includes nine nodes. Total mass flux is calculated separately in the four zones around the central node (Fig. 2). The film thickness, velocity and pressure (for Poiseuille flow) are defined at nodes and are linearly interpolated within each zone. In agreement with Eq. (2), total flux in each node must equal zero

$$Q = Q_P + Q_C = 0. \tag{7}$$

The Poiseuille flow Q_P is similar with one, considered by Kawabata [1] and will not be expanded here. The Couette flow

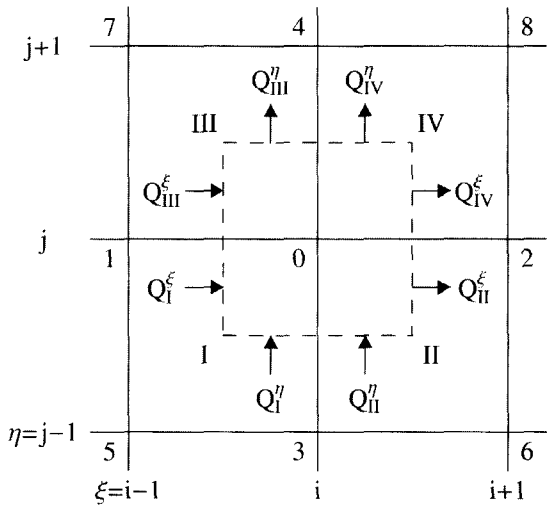

Fig. 2. Total flux for node (i, j).

Q_C is considered in details in the next section.

Couette Flow Calculation

In the BFCS method with upstream scheme [1], the total Couette flow is expressed as follows

$$Q_C = \frac{1}{8} \sum_{i=0}^{8} a_i P_i, \tag{8}$$

where

$$a_0 = 3(D_I^- - D_{II}^+ + D_{III}^- - D_{IV}^+ + E_I^- + E_{II}^- - E_{III}^+ - E_{IV}^+), \tag{9}$$

$$\begin{aligned} a_1 &= 3(D_I^+ + D_{III}^+) + E_I^- - E_{III}^+, \\ a_2 &= -3(D_{II}^- + D_{IV}^-) + E_{II}^- - E_{IV}^+, \\ a_3 &= D_I^- - D_{II}^+ + 3(E_I^+ + E_{II}^+), \\ a_4 &= D_{III}^- - D_{IV}^+ - 3(E_{III}^- + E_{IV}^-), \end{aligned} \tag{10}$$

$$\begin{aligned} a_5 &= D_I^+ + E_I^+, \\ a_6 &= -D_{II}^- + E_{II}^+, \\ a_7 &= D_{III}^+ - E_{III}^-, \\ a_8 &= -D_{IV}^- - E_{IV}^-, \end{aligned} \tag{11}$$

and D^+, D^-, E^+ and E^- are defined as follows

$$\begin{aligned} &D^+ = 0.5(D + \lambda|D|), \\ &D^- = 0.5(D - \lambda|D|), \\ &E+ = 0.5(E + \lambda|E|), \\ &E^- = 0.5(E - \lambda|E|). \end{aligned} \tag{12}$$

When the upstream coefficient, λ, is zero, $D^+ = D^- = 0.5D$, $E^+ = E^- = 0.5E$, and Eqs. (9-11) correspond to the Couette flow terms (Eq. (5)), that was integrated with linearly interpolated pressure. In such scheme, the coefficient of P_0, i.e. a_0, can become positive (Eq. (9)). Since D and E are proportional to the compressibility number Λ (see Eq. (6), increasing Λ can

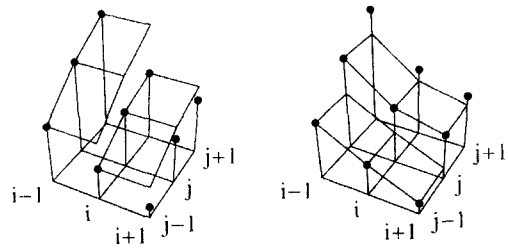

Fig. 3. Original BFCS. Interpolating function in Couette flow term. (a) -ξ-direction, (b) -η-direction.

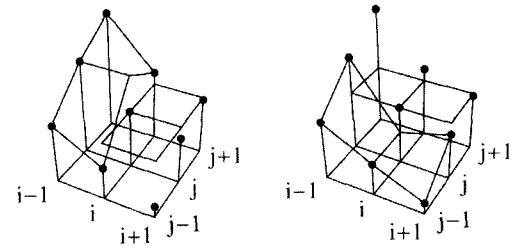

Fig. 4. Modified BFCS. Interpolating function in Couette flow term. (a) -ξ-direction, (b) -η-direction.

result in positive coefficient of P_0 in the total flux (Eq. (7)). In this case, the nodal pressure is alternating and the solution is wavy.

When the upstream coefficient, λ, achieves unit, we have fully upstream scheme with $D^+ = D$, $D^- = 0$, $E^+ = E$ and $E^- = 0$. In this case, Eqs. (9-11) correspond to the Couette flow terms that was integrated with pressure interpolation same as in Fig. 3. We can see (Eq. (9)), that in this case, the coefficient of P_0 is strictly negative, thus the alternating, wavy solution is avoided. In low compressibility number region the full upstream scheme produce inaccurate solution with so called "false diffusion" [3].

However, as we can see from Eq. (10), ξ-direction dominant flow can result in negative values of a_3 and a_4, as well as η-direction dominant flow can result in negative values of a_1 and a_2. Thus, waviness in direction, perpendicular to the disk surface velocity, can be expected.

In order to eliminate this kind of artificial waviness, the pressure distribution, as shown in Fig. 4 for fully upstream scheme, was substituted to the integrals (5). The coefficients of Eq. (8) were modified as follows

$$a_0 = 4(D_I^- - D_{II}^+ + D_{III}^- - D_{IV}^+ + E_I^- + E_{II}^- - E_{III}^+ - E_{IV}^+), \quad (13)$$

$$a_1 = 3(D_I^+ + D_{III}^+) + 0.5(E_I^+ - E_{III}^-),$$

$$a_2 = -3(D_{II}^- + D_{IV}^-) + 0.5(E_{II}^+ - E_{IV}^-),$$

$$a_3 = 0.5(D_I^+ - D_{II}^-) + 3(E_I^+ + E_{II}^+),$$

$$a_4 = 0.5(D_{III}^+ - D_{IV}^-) - 3(E_{III}^- + E_{IV}^-), \quad (14)$$

$$a_5 = 0.5(D_I^+ + E_I^+),$$

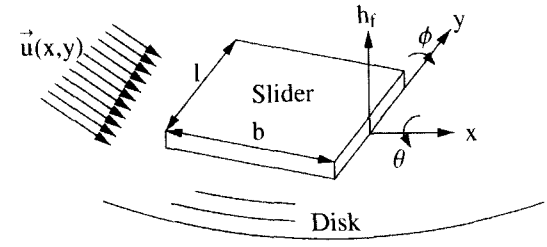

Fig. 5. The position of slider above the disk.

$$a_6 = 0.5(-D_{II}^- + E_{II}^+),$$

$$a_7 = 0.5(D_{III}^+ - E_{III}^-),$$

$$a_8 = 0.5(-D_{IV}^- - E_{IV}^-), \quad (15)$$

In this case, the central node coefficient is strictly negative (13) and the diagonal nodes coefficients are strictly positive (15), as before, and the coefficients a_1, a_2, a_3 and a_4 are also strictly positive, so, no arti.cial waviness can be expected for the fully upstream scheme. The inaccuracy introduced to the solution by this modification is expected to be of the same order with one, introduced by original fully upstream scheme. However, numerical experiments are required to show that the solution remains the same for low compressibility number values.

Steady State Position

The slider has three degrees of freedom: vertical motion, pitching and rolling. The corresponding position components are called flying height, h_f, pitching angle, ϕ, and rolling angle, θ (Fig. 5).

The position of the slider and its surface shape h_S (X, Y) define the distribution of the air film thickness between the slider and the disk surface

$$H(X, Y) = (h_S(x, y) + h_f + \phi(b - x) + \theta(l/2 - y))/h_0. \quad (16)$$

As was mentioned before, the pressure distribution $P(X, Y)$ is related to the film thickness $H(X, Y)$ (see Eq. (1)). Hence, the slider position defines the pressure distribution for given slider surface shape, disk rotation speed and radial position of the slider.

Total vertical force, pitching moment and rolling moment consist of the air bearing pressure resultant force and moments and the action of the preload force W, applied at the point (x_p, y_p).

$$L(h_f, \phi, \theta) = -W + \int p dx dy, \quad (17)$$

$$M_\phi(h_f, \phi, \theta) = W(x_p - b/2) - \int p(x - b/2) dx dy, \quad (18)$$

$$M_\theta(h_f, \phi, \theta) = W(y_p - l/2) - \int p(y - l/2) dx dy. \quad (19)$$

In the steady state position of the slider the total force and moments should equal zero

$$(L, M_\phi, M_\theta) = (0, 0, 0). \quad (20)$$

In the present work, the steady state position is determined

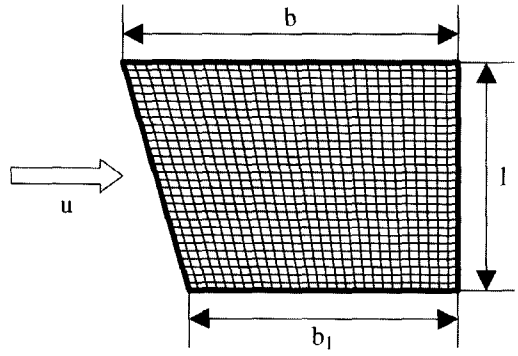

Fig. 6. Skewed slider.

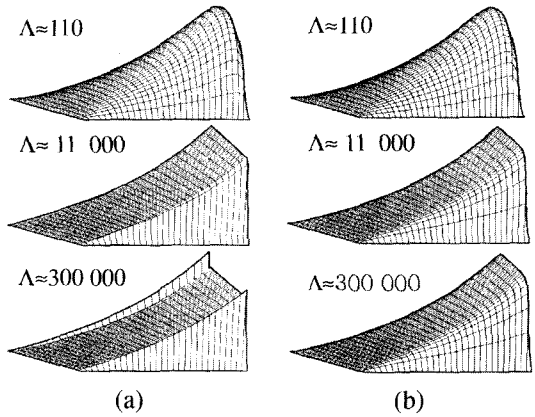

Fig. 7. Pressure distribution for skewed slider. (a) -Original BFCS, (b) -Modified BFCS.

Table 1. Skewed slider parameters

b	l	b_1	u
3 mm	2 mm	2.4 mm	20 m/sec

by using the search algorithm, based on the optimization approach [7].

Computational Test

The original and modified methods were used to calculate the pressure distribution for skewed slider (Fig. 6). The parameters of the skewed slider are given in Table 1. Minimum film thickness, that is the same as the flying height and the base film thickness in this example, takes the values 800, 80, 15 nm. Corresponding values of the compressibility number approximately equal 110, 11,000 and 300,000. The pitching angle is chosen to provide $h_{max}/h_{min} = 2$ for all values of h_{min}.

Figure 7 shows that the pressure distribution, calculated by original BFCS DF method, becomes discontinuous at higher values of Λ, while the modified methods provides smooth solution. As could be expected, the waviness appear only in the transverse direction. Note, that for smaller Λ both methods give identical results.

Femto-Slider Analysis

The modified BFCS with fully upstream scheme was applied for static analysis of the femto-slider [8].

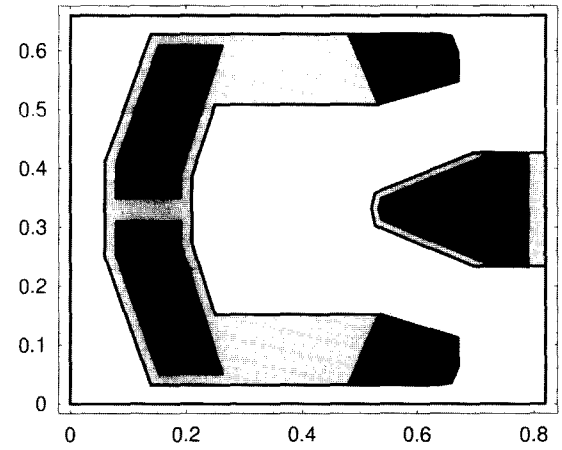

Fig. 8. Air bearing surface of the femto-slider.

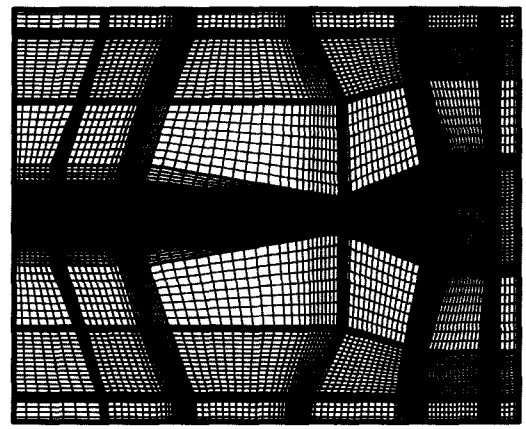

Fig. 9. Mesh for the femto-slider analysis.

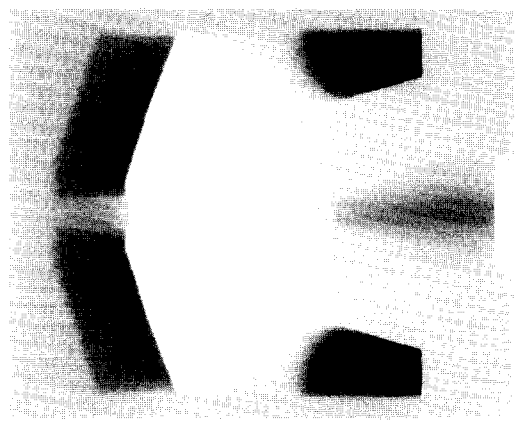

Fig. 10. Pressure distribution of the femto-slider.

For this slider, $b = 0.88$ mm and $l = 0.66$ mm. The recess depths of the base and shallow levels are 2,500 nm and 300 nm correspondingly (see Fig. 8). The pivot preload amounting 0.5 gf is applied at the slider center. The disk rotation speed is 7,200 rpm and the slider is positioned 15 mm far from the disk center. Typical values of the compressibility number fall in the range (350,000; 450,000).

The mesh that was used for the femto-slider analysis is

Table 2. Steady state position of the femto-slider

Crown (nm)	h_f (nm)	ϕ (μrad)	θ (μrad)
0	4.5	27	3.4
18	8	72	3

shown in Fig. 9. The grid lines are fitted to the pads' and recesses' boundaries. The mesh is refined in the areas where high pressure gradients are expected.

The static characteristics were estimated for two modification of the femto slider: one with flat zero recess level and another one with significant crown. The results are given in Table 2.

The results show that the crowned slider has bigger flying height and bigger pitching angle.

The pressure distribution for crowned slider in the steady state position is shown in Fig. 10. We can see the high pressure at the leading pads and rail pads, lower pressure at the trailing edge and the subambient pressure in the central cavity.

Conclusions

The modification of the Couette flow terms in the BFCS DF method is proposed. The modified method eliminates the artificial waviness in transverse direction, preserving the accuracy of the original method. However, it is subject to false diffusion in the same way as original fully upstream scheme. Thus, this method is specialized for solution of the Reynolds equation with extremely high compressibility numbers.

The static characteristics of the femto-slider are studied using the modified BFCS DF method. The analysis results show that increasing air bearing crown increased the steady state flying height and pitching angle.

Acknowledgment

The authors would like to appreciate the financial support provided for continuing this research by Yeungnam University Brain Korea 21 support program.

References

1. N. Kawabata, A Study on the Numerical Analysis of Fluid Film Lubrication by the Boundary-Fitted Coordinates System (The Case of Steady Gas-Lubrication) JSME Int. J, SR-III, Vol. 32, No. 2, pp. 281-288, 1989.
2. B. J. Hamrock, Fundamentals of Fluid Film Lubrication, p. 330, McGraw-Hill, Singapore, 1994.
3. S. V. Patankar, Numerical Heat Transfer and Fluid Flow, pp. 79-112, McGraw-Hill, USA, 1980.
4. L. Wu and D. B. Bogy, Use of an Upwind Finite Volume Method to Solve the Air Bearing Problem of Hard Disk Drives, Computational Mechanics, Vol. 26, pp. 592-600, 2000.
5. A. N. Brooks and T. J. R. Hughes, Streamline Upwind/ Petrov-Galerkin Formulations for Convection Dominated Flows with Particular Emphasis on the Incompressible Navier-Stokes Equations, Computer Methods in Applied Mechanics and Engineering, Vol. 32, pp. 199-259, 1982.
6. N. Kawabata, Numerical Analysis of Reynolds Equation for Gas Lubrication in High Λ Region), JSME Int. J, SR-III, Vol. 30, p. 836, 1987.
7. P. Hwang and P. V. Khan, Application of Optimization Approach to Static FE Analysis of HDD Slider, Proceedings of 2004 ASME/STLE Joint International, Long Beach, USA, 2004.
8. L. Wu, and D. B. Bogy, Effect of the Intermolecular Forces on the Flying Attitude of Sub-5 NM Flying Height Air Bearing Sliders in the Hard Disk Drives, ASME J. of Trib., Vol. 124, pp. 562-567, 2002.